MULTI-OBJECTIVE OPTIMIZATION IN DECIDING VESSEL NAVIGATION SPEEDS AND EMISSION CONTROL MEASURES FOR ARCTIC SHIPPING

Chathumi Ayanthi KAVIRATHNA[1], Ryuichi SHIBASAKI[1], Wenyi DING[2], Natsuhiko OTSUKA[3]

1 Researcher, Resilience Engineering Research Center, The University of Tokyo, Tokyo, Japan
E-mail: chathumiayanthi@gmail.com
1 Associate Professor, Resilience Engineering Research Center, The University of Tokyo, Tokyo, Japan
E-mail: shibasaki@tmi.t.u-tokyo.ac.jp
2 Graduate Student, Department of Systems Innovation, The University of Tokyo, Tokyo, Japan
E-mail: ding-wenyi@g.ecc.u-tokyo.ac.jp
3 Professor, Arctic Research Center, Hokkaido University, Hokkaido, Japan
E-mail : natsuhiko.otsuka@arc.hokudai.ac.jp

Significant attention on Arctic shipping in recent years caused by global warming and retreat of sea ice encourages growth in the number of vessels transit via the Northern Sea Route (NSR). However, the fragile environment of the Arctic Sea would experience significant environmental concerns due to the vessel-based emissions from navigation activities. Therefore, enforcement of different emission control measures (ECMs) would be significant to ensure the environmental sustainability of Arctic shipping. However, considering the economic feasibility of Arctic shipping, ECMs should be decided with both environmental and economic objectives. Although navigation speed has substantial impacts on Arctic shipping, not many studies focused on both environmental and economic aspects simultaneously for optimizing navigation speeds. Therefore, this study develops a multi-objective mixed-integer non-linear optimization model to decide optimum vessel speeds and locations of heavy fuel oil (HFO)-banned areas for a given voyage. Moreover, three scenarios are considered given as free ice, medium ice, and heavy ice incorporating the ice condition along navigation paths. According to the results, a significant reduction of vessel-based emissions is observed than the status quo due to the proposed speed optimization and HFO-banned areas. Moreover, the minimizing cost objective tends to have comparatively higher speed and shorter voyage duration while minimizing emissions objective supports the slow steaming strategy to reduce fuel consumptions and emission level. Furthermore, heavy ice condition drives comparatively higher average speed than the free ice and medium ice conditions. The selected HFO-banned areas are significantly different when changing the ice conditions even with the same environmental or economic objective.

Key Words: *Multi-objective, Speed optimization, Vessel-based emissions, Arctic Shipping, Emission control measures*

1. INTRODUCTION

The continuous retreat of sea ice driven by global warming develops a new avenue for the global shipping market with a focus on Arctic shipping. The Northern Sea Route (NSR) has the potential to facilitate a more economical cargo movement between Asia and Europe, than conventional shipping routes (Cariou and Faury, 2015; Kavirathna and Shibasaki, 2021; Stephenson et al., 2013; Xu et al., 2011). NSR is a shipping lane between the Atlantic and the Pacific Ocean along the Russian coast of Siberia and Far East, and this route extends via five Arctic seas namely, Barents Sea, Kara Sea, Laptev Sea, East Siberian Sea, and Chukchi sea (Liu and Kronbak, 2010). Despite the economic advantages, Arctic shipping may result in serious environmental concerns due to the vessel-based emissions generated from navigating vessels. Therefore, different operation- and policy-based measures must be considered to minimize vessel-based emissions to the Arctic Sea environment. However, when deciding on these emission control measures (ECMs), both environmental and economic objectives must be addressed simultaneously without violating the economic feasibility of NSR (Ding et al., 2020; Theocharis et al., 2019).

ECMs can be either operation-based or policy-based measurers and could have various impacts on the Arctic shipping potential. Thus, this study analyzes the effectiveness of two ECMs; speed optimization which is an operation-based measurer, and heavy fuel oil (HFO)-banned areas which is a policy-based measurer to conform sustainability of Arctic shipping from both environmental and economic perspectives. Owing to the non-linear relationship between a vessel's speed and her fuel consumption, speed optimization would play a vital role in minimizing emissions and costs associated with voyages (Otsuka et al., 2013). Moreover, HFO-banned areas help in limiting vessel-based emissions by limiting the burning of HFO inside these areas and switching to more environmentally friendly fuel types with lower emission factors of greenhouse gasses (Theocharis et al., 2019). This study incorporates HFO-banned areas due to the ongoing discussion on enforcing HFO-banned areas along the NSR. When considering HFO-banned areas, it is assumed that vessels are required to switch from HFO to marine gas oil (MGO), which is a more environmentally friendly fuel type (IMO 2020) when navigating through these HFO-banned areas.

Therefore, the objectives of this study are as follows. First, we estimate the emissions and cost of the voyage without ECMs when navigating via NSR. Second, we analyze the optimum speed and the locations of HFO-banned areas to minimize total cost under a restricted emission level. Third, we analyze the optimum speed and the locations of HFO-banned areas to minimize total emissions under a restricted cost level. To achieve these research objectives, a multi-object non-linear optimization model is considered with the ἐ constrained method to optimize the navigation speeds of vessels and the location of HFO-banned areas considering individual voyages. Both economic and environmental objectives are analyzed individually considering the remaining objective as a constrain. When estimating emissions, total carbon dioxide equivalent (CO2e) is estimated as a function of CO2, CH4, N2O, and black carbon (BC) emissions. Finally, the effectiveness of proposed ECMs is discussed in comparison to the status quo which does not consider any ECMs for the NSR.

In contrast to the conventional shipping routes, navigation via NSR is greatly affected by the sea-ice condition. To incorporate the impacts of ice-condition, we analyze the effect of ECM under three ice-condition scenarios given as free-ice (Aug-Sep), medium-ice (Oct-early Nov), and heavy-ice (late Nov-Dec) which depend on the navigation time of the year. Thus, optimized speeds and locations of selected HFO-banned areas are obtained at three ice conditions and compared to understand the effects of sea-ice conditions for the environmental and economic aspects of Arctic shipping.

As the remainder of this paper, Section 2 provides a literature review and Section 3 discusses the multi-objective optimization model. Section 4 describes the model application and focuses on the results and discussion. Finally, Section 5 provides the conclusions along with future research directions.

2. LITERATURE REVIEW

This section summarizes the previous studies related to speed optimization, environmental and economic aspects of Arctic shipping, and ECMs for Arctic shipping as follows.

Regarding speed optimization, an extensive number of studies focused on speed optimization of vessels with different objectives and approaches. As for the speed optimization model, Fagerholt and Psaraftis (2015) developed two-speed optimization problems for ships that sail in and out of EC areas with different fuel types and obtained significantly different speeds inside and outside EC areas. Kim et al. (2016) analyzed a speed optimization problem for minimizing the total fuel consumption and considered multiple time windows with each port call as constraints. A speed optimization model with a loss aversion mechanism was proposed by Zhao et al. (2020) and considered the trade-off relationship between fuel consumption, SOx emissions, and delays of the voyage. The proposed model was effective in analyzing slow steaming risk-based decisions of shipping lines. Ma et al. (2020) developed a route and speed optimization model which minimizes time and cost and incorporates EC areas. The proposed model could reduce the time and cost of the voyage and help shipping companies to deal with the variation of fuel prices.

Summarizing a few selected studies that focused on environmental and economic feasibility of NSR, Zhang et al. (2018) assess the exploitation of trans-Arctic routes incorporating sea-ice evolution with a big data mining approach. They calculated ice numeral and safe navigation speed based on estimated sea ice concentration, sea ice extent, and ice thickness, and then estimated navigation time and cost. Furthermore, to analyze the climate and economic feedback of NSR, Yumashev et al. (2017) considered two climate change scenarios given as high emissions and medium mitigation levels. The navigability of NSR is determined based on predicted ice conditions and then fed into a business model to determine NSR's profitability. Furthermore, Stephenson et al. (2013) analyzed the technical shipping accessibility to the Arctic sea areas for the 21st century. They simulated maritime access considering the ice-breaking capability of vessels and ice conditions along the route and highlighted that Polar Class 3 (PC3), PC6, and open-water vessels would experience accessibility to the 95 %, 78 %, and 49 % areas of Arctic, and their July-October navigation season length via NSR averages 120, 113, and 103 days, respectively. By analyzing daily ice thickness data from 2006 to 2016 for 49 subzones along NSR, Cariou et al. (2019) derived vessel speed based on ice condition and compared the cost of NSR with that of the Suez Canal route and Trans-Siberian railway connection. According to the results, a higher CO2 emission per TEU was highlighted for the NSR than the Suez Canal route due to a gap between the vessel's design and operating speeds.

Next, previous studies related to ECMs on Arctic shipping are summarized as follows. Accordingly, Ding et al. (2020) analyzed the feasibility of NSR against SCR considering the fixed vs. progressive carbon tax schemes with alternative fuel choices. As per the results, NSR is viable when enforcing/not enforcing carbon tax in both routes simultaneously despite the fixed or progressive tax schemes. Theocharis et al. (2019) incorporated environmental policy for promoting the transition from high to low sulfur fuels with a speed optimization model that minimizes the required freight rate between NSR and SCR. Accordingly, despite the decrease in fuel cost, capital and operating costs tend to be increased due to the longer duration of the voyage caused by a speed that is slower than the optimal one. The competitiveness of NSR for bulk shipping was investigated by Cariou and Faury (2015) while deciding the optimal speed to maximize short-term daily profits along with a future environmental policy on CO2 emissions. Accordingly, NSR was competitive than SCR when an environmental policy is implemented with a high carbon tax. NSR's competitiveness was further increased when increasing the SCR's speed because fuel-saving becomes significant. The effectiveness of speed optimization, bunker levy, and speed limits was analyzed by Psaraftis (2019), and results highlighted several deficiencies with the speed limit option as a measurer to reduce GHG emissions.

In summary, despite the availability of previous studies in analyzing the Arctic shipping feasibility, the majority of them obtained results assuming an average speed for the entire route while excluding the effect of spatial and temporal variation in ice conditions. Moreover, studies made simplified assumptions on ice-breaking cost, emission tax, and fuel consumption, among others. The majority of studies considered seven zones of NSR for the convenience of estimating cost while excluding detailed geometry along the navigation path. A very few studies incorporated ice conditions along the navigation path when analyzing economic and environmental feasibility. Most previous studies that focus on speed optimization considered optimum speed for the entire route and do not consider optimum speeds at small navigation legs considering the variation of their ice conditions. Therefore, this study develops a multi-objective optimization model considering both economic and environmental objectives and decides optimum speeds and locations of HFO-banned areas. Detailed routing geometry with small navigation legs are considered to incorporate spatial-temporal variations of ice conditions and ice-breaking fees are estimated with ice conditions along the navigation paths. To estimate fuel consumption, an approach similar to the IMO fourth GHGs emission study is considered, and emissions levels are estimated with multiple GHGs. Although previous studies considered EC areas and speed optimization focusing on other shipping routes, not many studies focus on such ECMs for the Arctic shipping routes. Therefore, this study focuses on speed optimization and HFO-banned areas as the operation-based and policy-based measurer on Arctic shipping. Hence, this study makes a significant contribution by revealing a method to identify the potential HFO-banned areas along the NSR for future environmental policy. Furthermore, considering of multi-objective optimization approach helps in the understanding effect of Arctic shipping from multiple perspectives.

3. METHODOLOGY

This section describes the development of a multi-objective optimization model including the methods for estimating the cost and emissions of the voyage.

(1) Voyage-specific navigation legs and HFO-banned areas

This study proposes a model to estimate voyage-specific optimum navigation speeds and optimum locations of HFO-banned areas. Specifically, individual navigation path of the vessel is extracted from vessel's automated identification system (AIS) data and divided into numerous navigation legs. In contrast to the previous studies that considered a few navigation legs and average vessel speed for all navigation legs, this study considers optimum speed in each navigation leg which is varied based on the spatial-temporal variation of ice condition. In this study, <=15nm and <=50nm are assumed as the thresholds for navigation length of each leg for the route segment within and outside NSR, respectively. Thus, the comparatively shorter length is maintained for the navigation legs within NSR than outside, thus speeds can be considered more precisely.

Before selecting the optimum locations of HFO-banned areas, the entire navigation area along the NSR is divided into 17 potential HFO-banned areas as given from A-Q in Fig. 1. In deciding potential HFO-banned areas, the area covering navigation paths of all transit vessels of NSR in 2017 and 2018 are considered. Although there can be many possible arrangements of potential HFO-banned areas, 17 areas are selected in this study considering factors such as distance from the coast (some boundaries are decided near the cost, some at a middle distance, and some far from the coast) and geographical highlights (e.g. Novaya Zemlya and Novosibirskiye Ostrova). As the ice condition inside each potential HFO-banned area is varied based on the time of the year, the optimum locations of selected HFO-banned areas could be varied depending on the time of the year. The total HFO-banned areas are limited to 17, so that one vessel may navigate through about 10 areas in a single transit at maximum

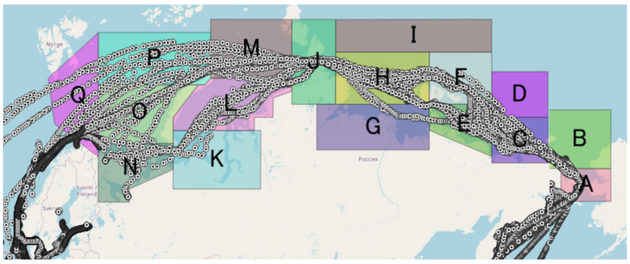

Fig.1 Potential HFO-banned areas.

(2) Ice-condition scenarios and navigation speeds

In contrast to the conventional shipping routes, navigation speed via NSR is greatly affected by the ice condition faced by the vessel. Thus, three different scenarios; free-ice, medium-ice, and heavy ice are assumed to incorporate the effect of different ice conditions. We obtain the daily ice thickness and ice concentration inside small grids along the respective navigation path from Arctic Data Archive-TOPAZ4 from 2018.07.01 to 2018.12.31 because this study focuses on the Summer–Autumn navigation season of NSR's transit vessels. To represent the ice condition, we multiply the daily ice thickness and ice concentration and obtain a five-day average ice condition. Thereafter, we generated an ice-condition distribution map along the navigation path as given in Fig.2, where the horizontal axis indicates the grid's location id given from left to right, and the vertical axis indicates the five-day average ice condition, thus higher values indicate more severe ice condition. Then, time-boundaries for free, medium, and heavy ice conditions are decided as per Fig.2 with actual ice conditions.

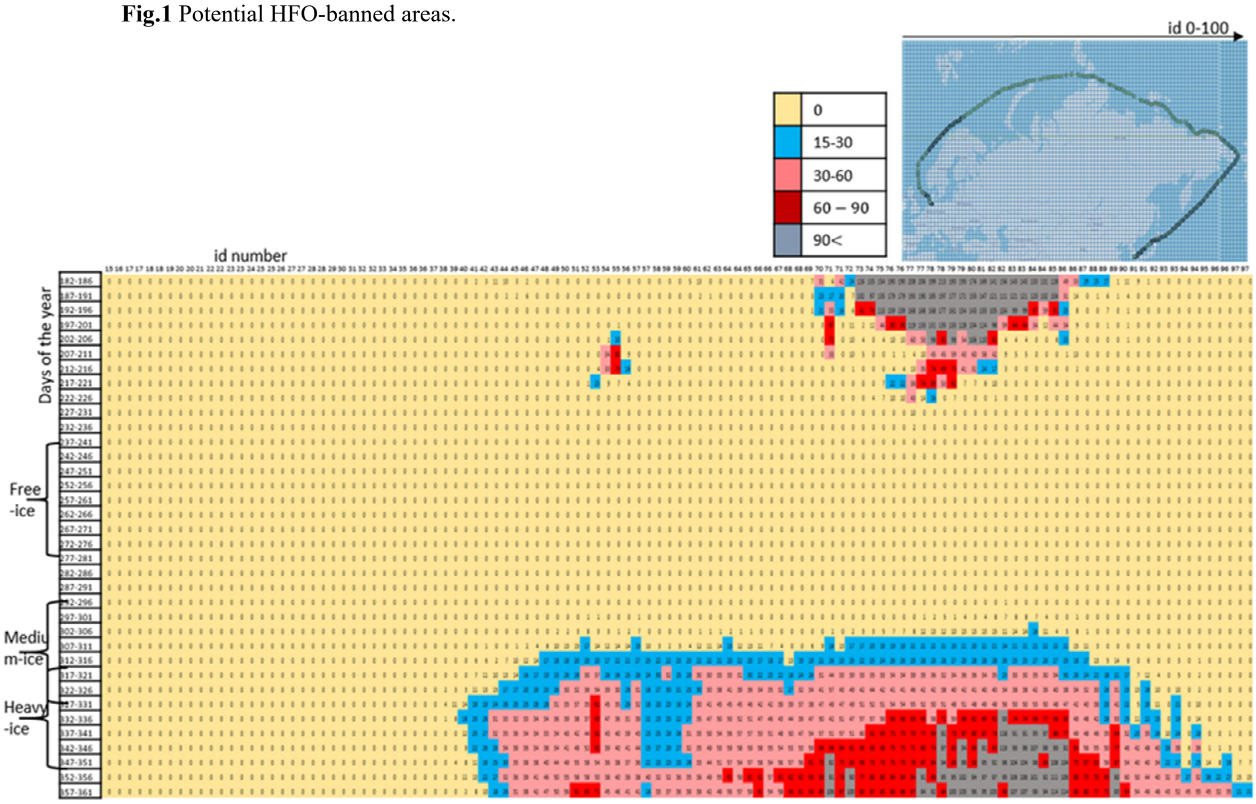

Fig.2 Scenarios based on ice condition.

Regarding navigation speeds, the speed with the status quo before optimizing is obtained from AIS data on the vessel's actual navigation trajectory at the free ice condition. The speeds at medium and heavy ice conditions are obtained based on the ice thickness at the respective vessel's position (leg l_n) at time t ($I_t^{l_n}$). Specifically, Equations (1) to (3) are used to estimate navigation speed based on ice thickness (Cariou et al., 2019). Four ice -thresholds I_i^1, I_i^2, I_i^3 and I_i^4 are assumed considering the vessel's ice-strength level. Descriptions on each ice-threshold level are given in Table 1.

Table 1 Navigation speed based on the ice condition.

Range	Description
$I_t^{l_n} < I_i^1$	Vessel i passing through the leg l_n can navigate without reducing speed
$I_i^1 < I_t^{l_n} < I_i^2$	Speed of vessel i has to reduce to a level defined by ice-thickness level (Equations 1-3)
$I_i^2 < I_t^{l_n} < I_i^3$	Vessel i needs icebreaker assistance and the speed of the ice-breaker equals 12 knots
$I_i^3 < I_t^{l_n} < I_i^4$	Vessel i passing needs icebreaker assistance and the speed of the ice-breaker equals 10 knots
$I_i^4 < I_t^{l_n}$	Vessel i cannot pass through leg l_n even with an ice-breaker

According to Table 1, the vessel can pass leg l_n independently without ice breaker assistance only if leg l_n's ice thickness is lesser than I_i^2 ($I_t^{l_n} < I_i^2$), thus has potential for optimizing speed. Otherwise, because the vessel needs ice-breaker assistance to pass leg l_n, this vessel's speed is assumed to be equal to the ice-breaker's speed. The variation of navigation speeds with ice conditions greatly influences the estimation of voyage cost and emissions.

$$S_{t,l_n,i}^{Max} = U \times \left(\frac{I_t^{l_n}}{100}\right)^V \tag{1}$$

$$U = S_i^d \times \left(\frac{100}{I_i^1}\right)^V \tag{2}$$

$$V = \{\log(S_i^{Min}) - \log(S_i^d)\}/\{\log(I_i^4) - \log(I_i^1)\} \tag{3}$$

where

N, l_n, i	Number of legs, n^{th} leg of the voyage, and i^{th} vessel passing through NSR
t	Time of the year (out of 365 days, t=1, 2, 3…365)
$I_t^{l_n}$	Ice thickness of the leg l_n at time t
$I_i^1, I_i^2, I_i^3, I_i^4$	Thresholds of ice thickness level for navigating of vessel i
S_i^{Min}, $S_{t,l_n,i}^{Max}$, S_i^d	The minimum speed, maximum speed, and design speed of vessel i
U, V	Vessel specific parameters

(3) Estimating cost and emissions of the voyage

The estimation of the total cost and emissions of the voyage for a multi-objective optimization model including both economic and environmental objectives is described as follows. Accordingly, the total cost is calculated by Equation (4) considering its four main components; capital cost, operating cost, fuel cost, and ice-breaking cost for a voyage. Capital and operating costs of the voyage are calculated by Equations (5) and (6), respectively (Xu et al., 2018). Here, σ and ρ indicate the premium for the new building price and additional operating cost of an ice-classed vessel compared to an open-water vessel.

The third component of Equation (4) represents the fuel cost which is calculated by Equation (7). Fuel cost is an important cost element of the speed optimization problem due to its non-linear relationship with the vessel's speed (IMO 2020). The total fuel cost is calculated as the summation of the individual leg's fuel consumption multiplied by the respective fuel price (HFO or MGO price). Since the fuel type burned during individual legs depends on whether they locate inside an HFO-banned area or not, δ_a^{HFO} equals to 1 if area a is an HFO-banned area and 0 otherwise. The total fuel consumption within a leg is estimated by Equation (8) considering the fuel consumption of the main engine, auxiliary engines, and boilers. Here, γ_{Auc} and γ_{Boi} indicate the fraction of time of using auxiliary engines and boilers from the total navigation time. In estimating fuel consumption, we incorporate criteria such as a ship's engine load, propulsive power demanded at different speeds, weather and fouling correction factors, auxiliary engines, and boilers, among others (IMO 2020). Thus, the admiralty formula for estimating the ship's main engine propulsive power demanded when she navigates at a given speed is calculated by Equation (9). Furthermore, Equation (10) calculates the specific fuel oil consumption of the main engine (SFC_{i,l_n}^{Main}) which is corrected from the engine load (EL_{i,l_n}) considering the parabolic variation of the SFC_{i,l_n}^{Main} as a function of its engine load (IMO 2020) and EL_{i,l_n} is given by $S_{t,l_n,i}^{Op}/S_i^d$ (Cariou et al., 2019).

In the navigation via NSR, ice-breaking cost also must be considered given as the last component of Equation (4). Equation (11) estimates the ice-breaking cost of the voyage which is applicable only for scenarios with medium and heavy ice conditions if the ice thickness level inside individual grids is in between I_i^2 and I_i^4. As per the NSR administration, this ice-breaking fee varies based on the vessel's GT, cost per GT per NSR's zone, and the required number of NSR's zones with ice-breaker assistance.

$$Cost_i = K_i + Oper_i + Fuel_i + IB_i \tag{4}$$

$$K_i = \frac{\sigma \times T_i^L \times Price_i^{NB}}{LT_i \times 365 \times 24} \tag{5}$$

$$Oper_i = \rho \times 0.5 \times K_i \tag{6}$$

$$Fuel_i = \sum_{n=1}^{N} \{\delta_a^{HFO} \times (F_{l_n,i} \times FP_{MGO}) + (1 - \delta_a^{HFO})(F_{l_n,i} \times FP_{HFO})\} \quad \forall l_n \in a \tag{7}$$

$$F_{l_n,i} = \{(SFC_{i,l_n}^{Main} \times P_{i,l_n}^{Main}) + (\gamma_{Auc} \times SFC_i^d \times P_i^{AuxEng}) + (\gamma_{Boi} \times SFC_i^d \times P_i^{Boi})\} \times (D_i^{l_n}/S_{t,l_n,i}^{Op}) \tag{8}$$

$$P_{i,l_n}^{Main} = \frac{\delta_w \times P_{ref,i}^{Main} \times (S_{t,l_n,i}^{Op}/S_i^d)^n \times (drf_{i,l_n}/drf_{ref,i})^m}{\eta_w \times \eta_f} \tag{9}$$

$$SFC_{i,l_n}^{Main} = SFC_{i,d}^{Main} \times (0.4551 \times EL_{i,l_n}{}^2 - 0.71 \times EL_{i,l_n} + 1.28) \tag{10}$$

$$IB_i = b_i \times B_n \times GT_i \tag{11}$$

where

$K_i, Oper_i, Fuel_i, IB_i$	Total capital cost, operating cost, fuel cost, and ice-breaking cost, respectively of vessel i for a given voyage
$Price_i^{NB}$ LT_i	Newbuilding price (USD) and lifetime (years) of vessel i
σ, ρ	Premiums on newbuilding price and operation cost respectively for ice-class vessels compared to an open-water vessel
$F_{l_n,i}$	Total fuel consumption by vessel i during leg l_n
$SFC_{i,d}^{Main}$, SFC_{i,l_n}^{Main}	Specific fuel oil consumption of the main engine (g/k Wh) of vessel i base value and when navigating inside leg l_n
EL_{i,l_n}	Engine load of vessel i when navigating inside leg l_n
$P_{ref,i}^{Main}$, P_{i,l_n}^{Main}	Reference power and power demanded by the main engine (kW) of vessel i at leg l_n
P_i^{AuxEng}, P_i^{Boi}	Power of auxiliary engines and boilers, respectively of vessel i
$\gamma_{Auc}, \gamma_{Boi}$	Fractions of time for using auxiliary engines and boilers from the total navigation time
$D_i^{l_n}$	Navigation distance of vessel i within the leg l_n for a given voyage
η_w, η_f	Weather and fouling correction factors
n, m	Relationship of vessel's required power with her speed and draught, respectively
$\gamma_{Auc}, \gamma_{Boi}$	Fractions of time for using auxiliary engines and boilers from the total navigation time
$drf_{ref,i}$, drf_{i,l_n}	Reference draft and the instantaneous draft of the vessel i at leg l_n
δ_w	Correction factor on the speed-power relationship
f, FP_f	Types of fuel (HFO, MGO) and price of fuel type f (USD/Ton)
$S_{t,l_n,i}^{Op}$	Optimum speed of vessel i during leg l_n at time t
a	HFO-banned areas; $a = A, B, \ldots\ldots, Q$
δ_a^{HFO}	Binary variable to decide whether area a is an HFO-banned area or not
B_n	Number of NSR's zones that require ice-breaker assistance
GT_i, b_i	Gross tonnage of vessel i and ice-breaking cost per NSR's zone per unit GT
B_n	Number of NSR's zones that require ice-breaker assistance

Apart from the cost of the navigation, this study also considers minimizing total emissions as an environmental objective. The total emission of the voyage is calculated by Equation (12) which incorporates multiple emission types (CO2, CH4, N2O, and BC) and their individual global warming potential values. Since we consider both HFO and MGO as fuel types when navigating outside and inside the selected HFO-banned areas respectively, individual emission factors of each emission type are considered.

$$Em_i = \sum_{e=1}^{4} \sum_{n=1}^{N} \{\delta_a^{HFO} \times (F_{l_n,i} \times EF_{MGO,e} \times \mathrm{GWP}_e) + (1 - \delta_a^{HFO})(F_{l_n,i} \times EF_{HFO,e} \times \mathrm{GWP}_e)\} \quad \forall l_n \in a \tag{12}$$

where

Em_i	Total emission from voyage (CO2e Tons)
e, $EF_{f,e}$	Emission type ($e = CO2, CH4, N2O, BC$) and emission factor of type e with fuel f
GWP_e	Global warming potential of emission type e

(4) Multi-objective optimization model

Based on the estimated total cost and emissions of the voyage, a multi-objective optimization model is developed to understand their tradeoff relationship and to derive policy implications. After testing with several alternative methods, the ε constrained method is considered for the multi-objective optimization model. Specifically, the model is run with two alternative objectives separately by converting the remaining objective as a constrain (ε). Equation (13) gives cost minimization objective with maximum allowable emission level, and Equation (14) gives emissions minimization objective with maximum allowable cost level, and these two objectives are considered to be alternative scenarios. As the variable to be optimized, the navigation speed varies between the minimum speed which is assumed based on the engine technology, and the maximum speed which is decided by the vessels' technical capabilities, ice conditions, navigation time of the year, etc. Equation (15) indicates these upper and lower bounds of vessel speed for the optimization. Note that since the maximum speed varies based on the vessel's entering time to a particular leg, the entering time is updated recursively incorporating optimum speed derived from the previous run until the new optimum speed does not vary further. Thus, For selecting the optimum locations for HFO-banned areas, Equation (16) gives a binary variable such that δ_a^{HFO} equals to 1 if area a is an HFO-banned area and 0 otherwise. Moreover, Equation (17) gives a constrain on the number of maximum allowable HFO-banned areas to test the model dynamics with having a restriction on the frequency of fuel switching. Finally, Equation (18) gives a constrain on total SOx emission as a fraction of total fuel consumption.

The model developed from Equation (1) to (18) is solved with the Frontline Solver 2020 version with its Evolutionary Solver feature that consists of both Genetic Algorithms and Tabu/Scatter search methods.

$$\min_{S_{t,l_n,i}^{Op},\delta_a^{HFO}} Cost_i \, , Em_i \leq \varepsilon_{emi} \tag{13}$$

$$\min_{S_{t,l_n,i}^{Op},\delta_a^{HFO}} Em_i \, , Cost_i \leq \varepsilon_{Cost} \tag{14}$$

$$S_i^{Min} \leq S_{t,l_n,i}^{Op} \leq S_{t,l_n,i}^{Max} \tag{15}$$

$$\delta_a^{HFO} = \{0,1\} \tag{16}$$

$$\sum_{a=1}^{M} \delta_a^{HFO} \leq A_{max} \tag{17}$$

$$\sum_{n=1}^{N}\{\delta_a^{HFO} \times (F_{l_n,i} \times EF_{MGO,SOx}) + (1 - \delta_a^{HFO})(F_{l_n,i} \times EF_{HFO,SOx})\} \leq \tau \times \left[\sum_{n=1}^{N}\{(\delta_a^{HFO} \times F_{l_n,i}) + (1 - \delta_a^{HFO}) \times F_{l_n,i}\}\right] \quad \forall l_n \in a \tag{18}$$

where

M Number of HFO-banned areas that a vessel is passing through during a given voyage

A_{max} The maximum allowable number of HFO-banned areas

τ Restriction on SOx emission as a fraction of total fuel consumption

ε_{emi}, ε_{Cost} Constraints on maximum allowable emissions and costs, respectively of the voyage

4. MODEL APPLICATION AND DISCUSSION

(1) Model application

The developed model is tested with a selected voyage which navigated from Busan to Bremerhaven made by Arc 4 class vessel. Table 2 describes the related vessel-specific, voyage-specific, model-specific, and market-specific input data of the voyage. The navigation path consists of 30 legs between its origin and NSR's entry point, 97 legs within NSR, and 20 legs between NSR's exit point and destination. The navigation path of the selected voyage is going through 11 HFO-banned areas within NSR (A, B, C, E, G, H, J, M, P, O, and Q).

Table 2 Input data for the model application.

Category	Inputs
Vessel- and voyage-specific data	GT: 34,882, LT_i: 10 years, $Price_i^{NB}$: 55,000,000 USD, $SFC_{i,d}^{Main}$: 170 g/k Wh, S_i^d: 19 knots, $P_{ref,i}^{Main}$: 31,808 k Wh, $drf_{ref,i}$: 11m, P_i^{AuxEng}: 1,400 KW, P_i^{Boi}: 430 KW, S_i^{Min}: 3 knots, I_i^1=0.1, I_i^2=0.3, I_i^3=0.6, I_i^4=0.9 m
Model-specific Parameters	σ: 1.1 (Otsuka et al., 2013), ρ: 1.25 (Zhang et al. (2016), Ding et al. (2020), η_f: 0.917 (IMO, 2020), n: 3 (IMO, 2020), η_w: 0.867 (IMO, 2020), δ_w: 1 (IMO, 2020), m: 0.66 m (IMO, 2020), γ_{Auc}: 50%, γ_{Boi}: 30%, A_{max}: 10
Market-specific Parameters	FP_{HFO}: 600 USD/Ton (Lindstad et al., 2016; Cariou et al., 2018), FP_{MGO}: 970 USD/Ton (Cariou et al., 2018), $\boldsymbol{e_{Tax}}$: 50 USD/Ton CO2e, τ: 0.04, Exchange rate: 1 USD equals to 75 RUB (https://www.cbr.ru), [GWP_{CO2} :1, GWP_{CH4} :28, GWP_{N2O}:265, GWP_{BC}: 900] (IMO, 2020), Emission factors (g/gfuel) [$EF_{HFO,CO2}$:3.114; $EF_{MGO,CO2}$:3.206; $EF_{HFO,CH4}$: 0.00006; $EF_{MGO,CH4}$:0.00006; $EF_{HFO,N2O}$:0.00016; $E_{MGO,N2O}$:0.00015; $EF_{HFO,BC}$: 0.00017; $EF_{MGO,BC}$:0.000004; $EF_{HFO,SOx}$:0.05083156; $EF_{MGO,SOx}$: 0.001368542] (IMO, 2020)

(2) Estimated results from the status quo

To understand the effect of speed optimization and HFO-banned areas, first, we obtain the results from the status quo without considering any ECMs. Note that the average speed of the free-ice scenario is obtained from AIS incorporating the vessel's actual navigation, and speeds at the medium and heavy ice scenarios are taken as the lowest value from the actual navigation speed and the speed given by the ice condition, which is derived from Equations (1) to (3) by incorporating vessel-specific characteristics and respective ice thickness level. Accordingly, Table 3 summarizes the average speed, total cost, and CO2e under the status quo with three ice condition scenarios. Thus, the medium-ice condition derives the least average speed for the voyage. This is possibly due to the significant drop of speed at the medium ice condition due to the presence of ice than the free-ice condition, Further, the vessel uses ice breakers in a significantly lower number of navigation legs at medium ice condition than the heavy ice condition, which results in slower independent navigation speed than the speeds with an ice breaker. Following the same trend, the least emission and cost levels are obtained from the medium ice scenario.

Table 3 Results from the Status Quo.

	Average speed (knot)	Total cost (Thousands USD)	CO2e (tons)
Free-ice	12.48	1458	4390
Mid-ice	12.22	1455	4310
Heavy-ice	12.47	1658	4388

(3) Average speeds obtained with the multi-objective optimization model

a) Minimizing total cost under each emissions constraint

This subsection summarizes the average speed decided from the multi-objective optimization model. Among multiple objectives including economic and environmental objectives, results obtained with minimizing cost objective are summarized in this subsection. Regarding the range for emissions constraint, the least possible CO2e level attainable under each ice condition is considered as the lower bound which gives the extreme level of restriction on CO2e emissions. However, there is no specific limit for the upper bound of the emission constraint as it can be extended further.

The average optimum speeds for each scenario on ice conditions are illustrated in Fig.3. Accordingly, if minimizing total cost and relaxing the emission constraint with higher allowable emissions levels, the average speed tends to be increased with all three ice conditions. However, there is a significant drop in the average speed of the voyage after the optimization under all three ice conditions compared to the status quo. It is reasonable to increase the speed if relaxing the emission constraint because of the positive relationship between vessel speeds and emissions levels. Since the objective is to minimize total cost, higher speeds are preferred to avoid the significantly high operations and capital cost associated with longer duration of voyages due to lower speed levels. Further, if comparing the results with three ice conditions, heavy and medium ice conditions indicate the highest and lowest average speed. The highest speed at heavy-ice conditions could be due to the usage of ice breakers. Further, at higher emissions constraint levels, both free and medium ice conditions tend to have a stable speed, possibly due to the inability to reduce the cost further by increasing speeds after this point.

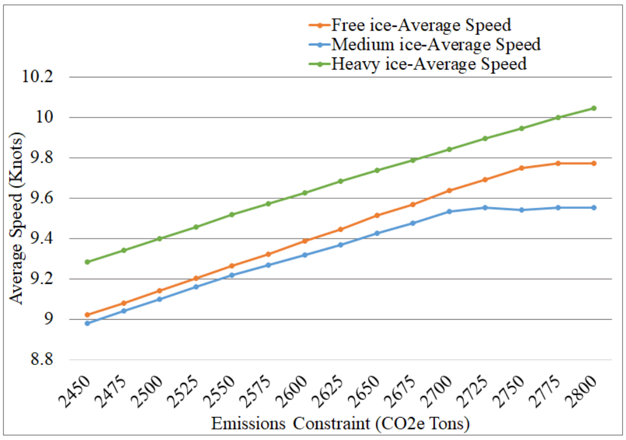

Fig.3 Average speeds under minimizing cost objective.

Fig.4 illustrates the variation of the economic objective under the variation of emission constraint for each ice condition which is plotted separately to understand their variation more clearly. Accordingly, if minimizing total cost under different values of emissions constraints, the average speed tends to be increased when relaxing emission constraint which eventually decreases the total cost. Therefore, within the given range of total emission level, slow steaming does not lower the total cost possibly due to the high operating and capital cost caused by additional days of the voyage despite the reduction in fuel cost at a slower speed. Further, heavy ice condition indicates the highest cost due to the extensive usage of ice breakers and inability to optimize speed because of being escourted by icebreaker in most navigation legs. Further, the costs associated with both free ice and medium ice conditions become fairly stable and do not decrease further at high values of emissions constraints due to their fairly stable vessel speed. However, under the heavy ice condition, the vessel operator has the potential to further reduce costs by emitting high emissions levels. Thus, enforcing a restriction on vessel-based emissions is very critical for the heavy-ice condition to ensure environmental sustainability. Similarly, heavy ice condition indicates a comparatively steeper reduction of total cost than free ice and medium ice conditions even with same values of emissions constraints.

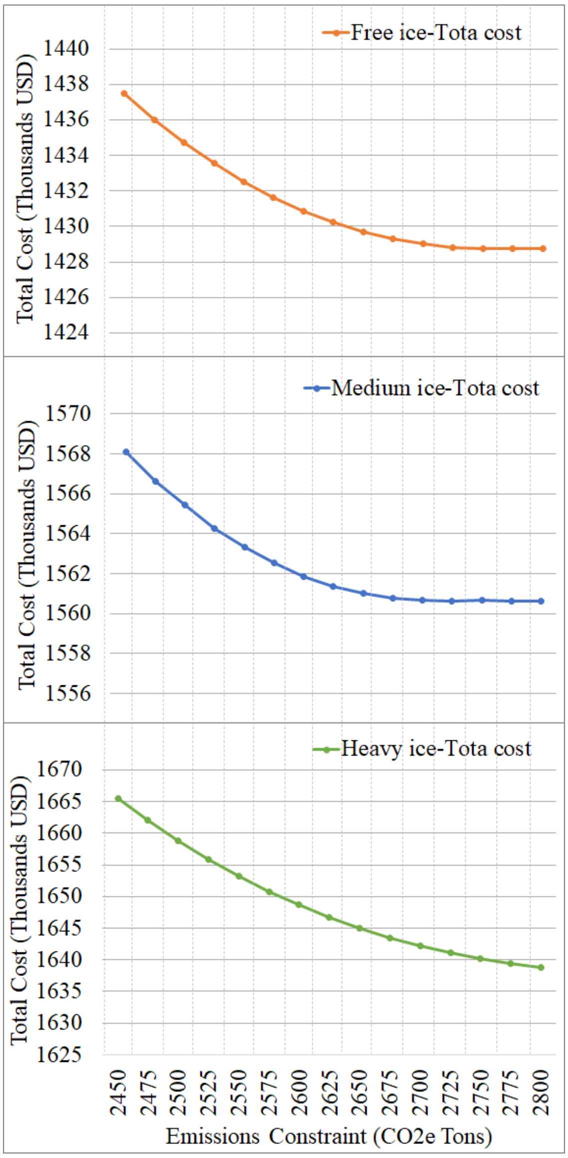

Fig.4 Estimated total costs under minimizing cost objective.

If comparing the total costs obtained from the optimization model and that associated with the status quo as shown in Table 3, in the free ice condition, a significant reduction in total cost as well as a significant lower emissions level is realized by speed optimization. However, under the medium and heavy ice scenarios, the possibility of having a lower cost than the status quo is greatly affected by the value of the emission constraint. For example, if we maintain a very restricted emissions level below 2500 CO2e tons as the emission constraint for the heavy ice scenario, then the proposed ECMs and optimization model would produce a higher total cost for the voyage than the cost at the status quo. However, this threshold value of 2500 CO2e tons is much lower than the total emissions produced at the status quo (4388.39 CO2e tons). In other words, there is a significant environmental benefit from proposed ECMs and thus policymakers should decide the effective level of restriction on voyage-based emissions which will generate both economic and environmental benefits.

b) Minimizing total emissions under cost constraint

This subsection summarizes the results if minimizing total emissions under a given cost constraint or maximum allowable cost levels. Fig.5 illustrates the variation of the average speed of the voyage at three ice condition scenarios if minimizing total emissions under given cost constraints. Accordingly, if allowing more costs for the voyage, the average speed tends to be decreased with all three ice conditions, indicating the potential of a slow steaming strategy to minimize the total emissions. This is reasonable due to the positive relationship between vessel-based emissions and navigating speeds, thus emissions can be minimized by slowing the speed. If comparing three ice-condition scenarios, the highest speed level is observed from the heavy ice scenarios due to the lower possibility of optimizing speeds at most navigation legs. However, if comparing to the minimizing cost objective, there is a significant difference in results for free ice and medium ice conditions if minimizing emissions. If minimizing cost, the speeds at free ice condition are higher than those at the medium ice condition; however, the slowest speeds are observed at the free ice condition in minimizing emissions. If minimizing cost, the trade-off between “fuel cost” and “operating and capital cost” would be considered which is affected by the vessel speed and voyage duration. Thus, a vessel may maintain a relatively higher speed at free ice condition if minimizing cost although the maximum possible speed under medium ice condition is restricted due to the presence of ice along the navigation route. However, if minimizing emissions, cost is considered only as a constraint, thus speed at free ice condition can be reduced further. Moreover, if comparing to the status quo and cost minimization objective, this emission minimization objective derives significantly slower optimum speeds.

Fig.6 highlights the relationship between emissions and cost levels if minimizing the total emissions. A clear trade-off relationship is observed between these two objectives, similar to the results obtained with minimizing cost objective as shown in Fig.4. If comparing results from three ice conditions, the lowest and highest emission levels are received from free-ice and heavy-ice conditions under the same cost constraint values, similar with the results shown in Fig.5. Further, if increasing the value of cost constraint, all ice conditions indicate a comparatively lower reduction of emissions than their emission reduction observed at lower values of cost constraint.

Accordingly, if minimizing emissions, by allowing additional cost for the voyage by relaxing the cost constraint, a significant reduction of emissions could be realized. However, it is important to consider the economic feasibility of Arctic shipping when deciding the acceptable maximum cost level by the vessel operators. Similarly, although there is an opportunity for vessel operators to minimize the total cost of the voyage by relaxing emissions constraints, allowing high emission levels from the vessel would result in devastating environmental impacts. Moreover, if comparing the results shown in Figs.3 and 5, minimizing emissions results in comparatively slower speed in general than minimizing cost objective. In summary, a clear tradeoff relationship could be observed between economic and environmental objectives.

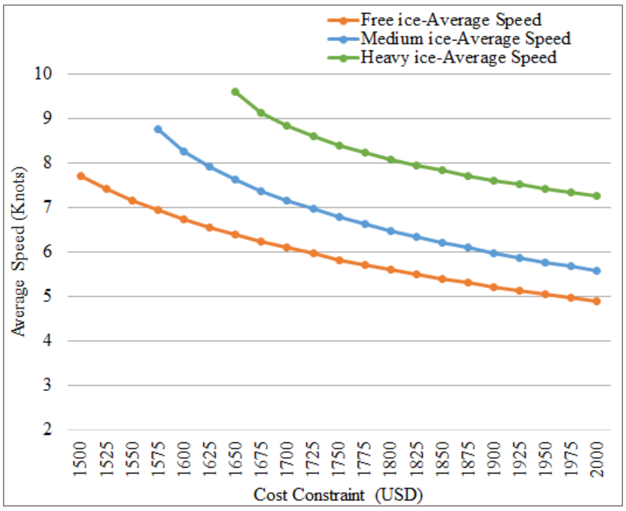

Fig.5 Average speeds under minimizing emissions objective.

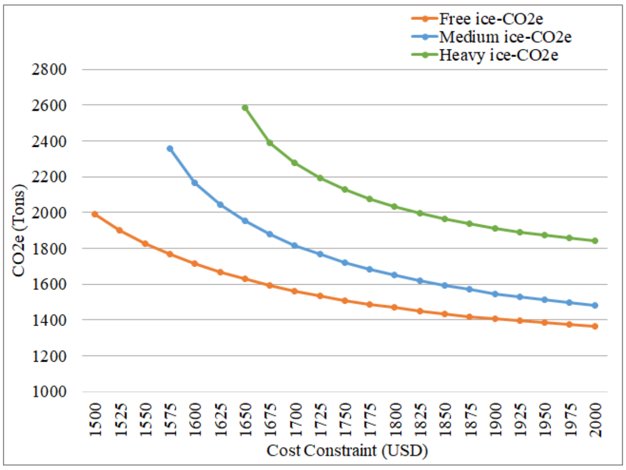

Fig.6 Estimated emissions under minimizing emissions objective.

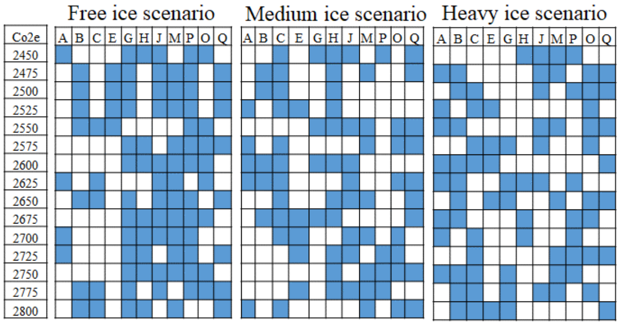

Fig.7 Selected HFO-banned areas under minimizing cost objective.

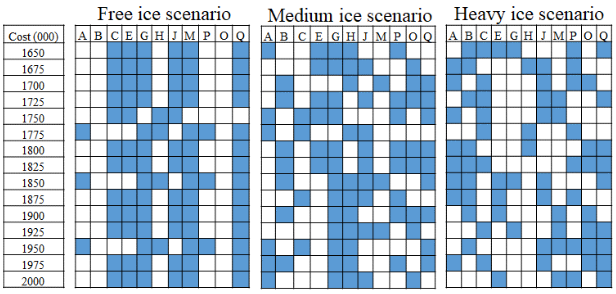

Fig.8 Selected HFO-banned areas under minimizing emissions objective.

c) Selected HFO-banned areas

Since this study focuses on selecting optimum locations of HFO-banned areas as well, the selected HFO-banned areas are summarized in Figs.7 and 8 by ice condition scenario considering minimizing cost and emissions objectives, respectively. In these figures, selected HFO-banned areas under each scenario are highlighted in blue color.

Accordingly, a significant difference of the selected HFO-banned areas is observed with two objectives and by ice conditions. Under the minimizing cost objective in Fig.7, areas such as P, M, and J are selected in most cases under free ice conditions, although those areas are not frequently highlighted under medium and heavy ice conditions. However, the selection of HFO-banned areas is greatly influenced by the navigation distances and average speeds of the vessel inside those areas.

Under the minimizing emissions objective in Fig.8, areas B and O are not selected as HFO-banned areas in the free ice condition although these areas are selected in the other two ice conditions. Moreover, areas C, E, G, J, M, and Q are selected as HFO-banned areas even if increasing the allowable cost level at the free ice condition. Although area G is mostly considered as an HFO-banned area under free ice and medium ice scenarios, it is rarely considered as an HFO-banned area under heavy ice condition. If selecting HFO-banned areas for the heavy-ice condition, usage of ice-breaking escorting service would have a significant impact due to the relatively higher speed of the ice breaker. For example, if the vessel has to escort an ice breaker inside a particular area, this area has a high potential to be selected as an HFO-banned area under the minimizing emissions objective because of the relatively higher vessel's speed when escorting an ice breaker and the positive relationship between vessel's speed and vessel-based emissions.

d) Duration of the voyage

Since we focus on a speed optimization problem, the duration of the voyage would be greatly affected by the optimum speeds with two optimization objectives and at different ice conditions. Therefore, the duration of the voyage when minimizing total cost and minimizing emissions are summarized in Fig.9 considering three ice conditions. In the figure, horizontal axis indicates the voyage duration obtained from the optimization model and the two vertical axes indicate the total cost obtained with cost minimization objective and total emissions obtained with emissions minimization objective. Accordingly, under the minimizing cost objective, the total cost tends to increase significantly with a longer duration of the voyage possibly due to higher capital and operating cost of the voyage. However, under the minimizing emissions objective, the total emission level tends to decrease if increasing the voyage duration. Thus, results of the minimizing emissions objective are generally associated with longer voyage durations than the minimizing cost objective.

Moreover, if comparing the results with three ice conditions, all three ice conditions indicate a similar pattern of variation of resulted cost and emissions associated with respective voyage durations. However, the free ice condition supports the extreme level of slow steaming, thus results in over 1500 hours of voyage duration. Meanwhile, the heavy ice scenario obtains less than 1300 hours of voyage duration with the emission minimization objective. Regarding the cost minimization objective, the total voyage duration does not exceed 900 hours under all three ice conditions, thus can be more realistic as the practical scenarios.

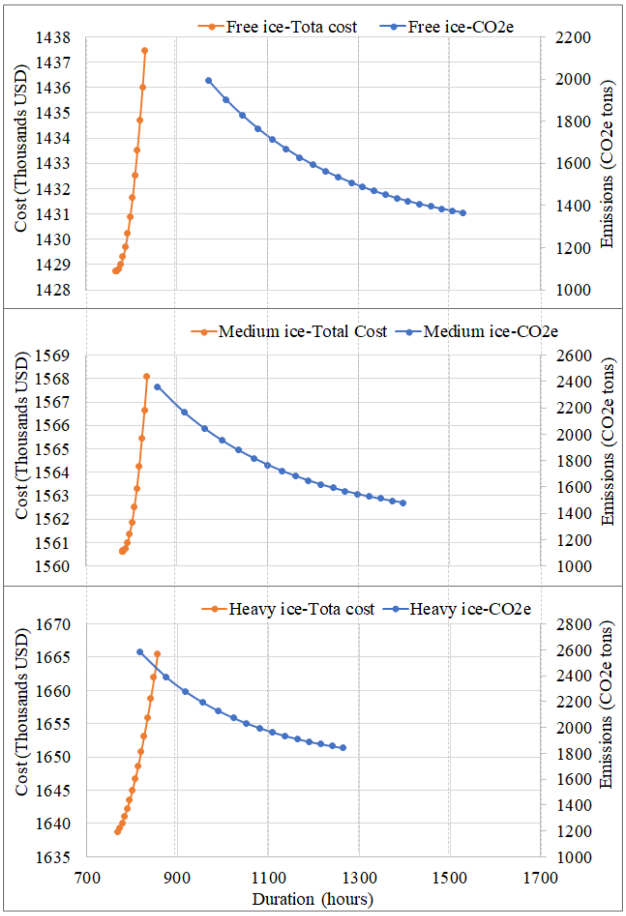

Fig.9 Voyage durations resulted from the optimization.

5. CONCLUSIONS

This study proposes a model for optimizing vessel speeds and locations of HFO-banned areas which are considered as the measurers for controlling vessel-based emissions from Arctic shipping. A multi-objective optimization model is developed with minimizing cost and minimizing emissions as two separate objectives and the ε-constrained method is used to solve the optimization problem. Three different scenarios; free-ice, medium-ice, and heavy ice are assumed considering the variation of ice condition along the navigation path and the time of the year. The benefits of speed optimization and HFO-banned areas are discussed in comparison to the status quo which has no ECMs.

In summarizing the main findings, a significant reduction of vessel-based emissions is observed under all three ice conditions than the status quo due to the proposed speed optimization and HFO-banned areas. Moreover, the proposed ECMs have the potential to reduce voyage costs than the status quo by enforcing an effective level of restriction on vessel-based emissions in deciding environmental policy. Voyage costs associated with medium and heavy ice conditions are generally higher than the free ice condition due to the cost of ice breakers and higher fuel consumption when navigating with ice-breaker assistance at a speed higher than the optimum speed. Moreover, when minimizing total cost and relaxing the emission constraint with higher allowable emissions levels, the average speed tends to be increased with all three ice conditions. Since the vessel operator has a high potential to reduce costs by generating high emissions levels under the heavy ice condition, enforcing a restriction on vessel-based emissions is very critical for the heavy-ice condition to ensure environmental sustainability. If allowing more costs for the voyage, the average speed tends to decrease with all three ice conditions, indicating the potential of a slow steaming strategy to minimize the total emissions. If compared to the status quo and the cost minimization objective, the emissions minimization objective derives significantly slower optimum speed. Moreover, a clear tradeoff relationship could be observed between economic and environmental objectives. The optimum speed and location of selected HFO-banned areas are significantly varied based on the ice condition.

As the limitations of this study, the arrangement of HFO-banned areas, navigation legs, and other input parameters have a significant influence on the results. Although this study suggests the optimum speeds for minimizing costs and emissions, it would be challenging to maintain such speeds at the individual navigation legs in the practical scenario because vessel speed would be affected by many other factors as well. In terms of future research directions, optimum locations of HFO-banned areas can be decided considering multiple voyages simultaneously, thus the implementation of such ECMs would be more realistic. Moreover, the model can be further developed considering speed optimization problems for NSR and alternative conventional shipping routes such as Suez Canal route simultaneously to discuss the economic feasibility of NSR with a more comprehensive approach.

REFERENCES

1) Cariou, P., and Faury. O.: Relevance of the Northern Sea Route (NSR) for bulk shipping. *Transp. Res. Part A*: Policy and Practice, 78, 337–346, 2015.
2) Cariou, P., Cheaitou, A., Faury, O., and Hamdan, S.: The feasibility of Arctic container shipping: the economic and environmental impacts of ice thickness. *Marit. Econ. Logist*, 2019.
3) Ding, W., Wang, Y., Dai, L., and Hu, H.: Does a carbon tax affect the feasibility of Arctic shipping?. *Transp. Res. Part D: Transport and Environment*, 80, 102257, 2020.
4) International Maritime Organization.: Fourth IMO GHG study, 2020.
5) Fagerholt, K., and Psaraftis, H.N.: On two speed optimization problems for ships that sail in and out of emission control areas. Transp. Res. Part D 39. 56–64, 2015.
6) Kavirathna, C.A., and Shibasaki, R.: Economic feasibility of Arctic shipping from multiple perspectives: a systematic review. Okhotsk Sea and Polar Oceans Research, 5, 15–22, 2021.
7) Kim, J., Kim, H., Jun H.B., and Kim, C.: Optimizing Ship Speed to Minimize Total Fuel Consumption with Multiple Time Windows, Mathematical Problems in Engineering, 2016.
8) Lindstad, H., Bright, R.M., and Strømman, A.H.: Economic savings linked to future Arctic shipping trade are at odds with climate change mitigation. *Transp. Policy*, 45, 24-30, 2016.
9) Otsuka, N., Izumiyama, K., and Furuichi. M.: Study on Feasibility of the Northern Sea Route from Recent Voyages. 22nd International Conference on Port and Ocean Engineering under Arctic Conditions. June 9–13, Espoo, Finland, 2013.
10) Psaraftis, H.N.: Speed Optimization vs Speed Reduction: the Choice between Speed Limits and a Bunker Levy. Sustainability, 11, 2249, 2019.
11) Stephenson, S.R., Smith, L.C., and 2 others.,: Projected 21st-century changes to Arctic marine access. *Clim. Change*, 118, 885–899, 2013.
12) Theocharis, D., Rodrigues, and 2 others.: Feasibility of the Northern Sea Route: The role of distance, fuel prices, ice breaking fees and ship size for the product tanker market. *Transp. Res. Part E: Logistics and Transportation Review*. 129, 111–135, 2019.
13) The ADS dataset is archived and provided by the Arctic Data archive System (ADS). National Institute of Polar Research. https://ads.nipr.ac.jp
14) Xu, H., Yang, D., & Weng, J.: Economic feasibility of an NSR/SCR-combined container service on the Asia-Europe lane: a new approach dynamically considering sea ice extent. *Marit. Pol. Manage*. 45(4), 514–529, 2018.
15) Xu, H., Yin, Z., & 3 others.: The potential seasonal alternative of Asia–Europe container service via Northern sea route under the Arctic sea ice retreat. *Marit. Pol. Manage*. 38:5, 541–560, 2011.
16) Yumashev, D., Hussen, K.V., and 2 others.: Towards a balanced view of Arctic shipping: estimating economic impacts of emissions from increased traffic on the Northern Sea Route. *Clim. Change*, 143, 143–155, 2017.
17) Zhang, Z., Huisingh, D., and Song, M.: Exploitation of trans-Arctic maritime transportation. *Journal of Cleaner Production,* 212, 960–973, 2018.
18) Zhang, Y., Meng, Q., and Ng, S.H.: Shipping efficiency comparison between Northern Sea Route and the conventional Asia-Europe shipping route via Suez Canal. . *J. Transp. Geogr*. 57, 241–249, 2016.
19) Zhao, Y., Zhou, J., Fan, Y., and Kuang, H.: Sailing Speed Optimization Model for Slow Steaming Considering Loss Aversion Mechanism. *Journal of Advanced Transportation*, 2020.